(1976).
(30) W. A. Lathan, W. J. Hehre, and J. A. Pople, *J. Am. Chem. Soc.*, **92**, 4796 (1970).
(31) L. Radom, W. J. Hehre, and J. A. Pople, *J. Chem. Soc. A*, 2299 (1971).
(32) L. Radom, W. J. Hehre, and J. A. Pople, *J. Am. Chem. Soc.*, **93**, 289 (1971).
(33) R. S. Mulliken, *J. Chem. Phys.* **23**, 1833 (1955).
(34) The substituents used were of the general type metal(alkyl)$_3$ or metal(phenyl)$_3$, which will have different electronegativities than those of the metal itself.
(35) E. Heilbronner and H. Bock, "Das HMO Modell und Seine Anwendung", Verlag Chemie, Weinheim/Bergstr., Germany, 1968, p 168.
(36) (a) M. J. S. Dewar, "The Molecular Orbital Theory of Organic Chemistry", McGraw-Hill, New York, N.Y., 1969; (b) W. L. Jorgensen and L. Salem, "The Organic Chemist's Book of Orbitals", Academic Press, New York, N.Y., 1973.
(37) Y. Apeloig, P. v. R. Schleyer, and J. A. Pople, *J. Org. Chem.*, to be published.
(38) J. D. Dill, P. v. R. Schleyer, and J. A. Pople, *J. Am. Chem. Soc.*, **99**, 1 (1977).
(39) (a) L. Radom, *Aust. J. Chem.*, **27**, 231 (1974). (b) For a recent experimental study see: G. A. Olah, A. Germain, and H. C. Lin, *J. Am. Chem. Soc.*, **97**, 5481 (1975).
(40) (a) W. A. Lathan, W. J. Hehre, and J. A. Pople, *J. Am. Chem. Soc.*, **93**, 808 (1971); (b) J. E. Williams, V. Buss, L. C. Allen, P. v. R. Schleyer, W. A. Lathan, W. J. Hehre, and J. A. Pople, *ibid.*, **92**, 2141 (1970).
(41) G. V. Pfeiffer and J. G. Jewett, *J. Am. Chem. Soc.*, **92**, 2143 (1970).
(42) (a) L. J. Massa, S. Ehrenson, and M. Wolfsberg, *Int. J. Quantum Chem.*, **4**, 625 (1970); (b) L. J. Massa, S. Ehrenson, M. Wolfsberg, and C. A. Frishberg, *Chem. Phys. Lett.*, **11**, 196 (1971).
(43) R. Sustmann, J. E. Williams, M. J. S. Dewar, L. C. Allen, and P. v. R. Schleyer, *J. Am. Chem. Soc.*, **91**, 5350 (1969).
(44) J. E. Douglas, B. S. Rabinovitch, and F. S. Looney, *J. Chem. Phys.*, **23**, 315 (1955).
(45) R. C. Bingham, *J. Am. Chem. Soc.*, **97**, 6742 (1975).
(46) L. Radom, W. J. Hehre, and J. A. Pople, *J. Am. Chem. Soc.*, **94**, 2371 (1972).
(47) J. D. Dill, P. v. R. Schleyer, and J. A. Pople, *J. Am. Chem. Soc.*, **97**, 3402 (1975).
(48) (a) N. L. Allinger and J. H. Siefert, *J. Am. Chem. Soc.*, **97**, 752 (1975); (b) G. A. Olah, *Angew. Chem., Int. Ed. Engl.*, **12**, 173 (1973); G. A. Olah, *J. Am. Chem. Soc.*, **94**, 808 (1972), and references cited therein.
(49) H. Nöth and B. Wrackmeyer, *Chem. Ber.*, **107**, 3089 (1974); B. F. Spielvogel, W. R. Nutt, and R. A. Izydore, *J. Am. Chem. Soc.*, **97**, 1609 (1975).
(50) J. Dill, Ph.D. Thesis, Princeton University, 1976, and unpublished results.
(51) Omitting the points for X = BH_2 and NH_2 from Figure 5 gives a line with a slightly improved correlation (r = 0.999) and a slope of 2.36.
(52) The optimized (RHF/STO-3G) C–C^+ and C–F bond lengths are 1.511 and 1.371 Å, respectively (from ref 8).
(53) A somewhat higher barrier was reported for X = F.[9] However, only the eclipsed form (**2**) was optimized, which artificially increases the barrier.[9]
(54) Y. Apeloig, P. v. R. Schleyer, and J. A. Pople, manuscript in preparation.
(55) (a) W. A. Lathan, W. J. Hehre, L. A. Curtiss, and J. A. Pople, *J. Am. Chem. Soc.*, **93**, 6377 (1971); (b) J. D. Swalen and J. A. Ibers, *J. Chem. Phys.*, **36**, 1914 (1962).
(56) The deficiencies of minimal basis sets for calculations involving lithium have been discussed by J. D. Dill, Ph.D. Thesis, Princeton University, 1976. A minimal basis for fluorine has a very small number of functions per electron and excessive energy lowering is obtained when vacant orbitals are introduced on the neighboring H_2C^+ group.
(57) The 4-31G and the extended double ζ basis sets[9] give similar rotation barriers for X = F (see also ref 53).

Organic Alloys: Synthesis and Properties of Solid Solutions of Tetraselenafulvalene–Tetracyano-*p*-quinodimethane (TSeF–TCNQ) and Tetrathiafulvalene–Tetracyano-*p*-quinodimethane (TTF–TCNQ)

E. M. Engler,* B. A. Scott, S. Etemad, T. Penney, and V. V. Patel

Contribution from the IBM Thomas J. Watson Research Center, Yorktown Heights, New York 10598. *Received December 6, 1976*

Abstract: The selenium analogues of tetrathiafulvalene (TTF), tetraselenafulvalene (TSeF) and diselenadithiafulvalene (DSeDTF), have been synthesized by trimethyl phosphite coupling of 1,3-diselenole-2-selone and 1,3-thiaselenole-2-selone, respectively. TTF, TSeF, and DSeDTF form isostructural. metallic charge-transfer salts with tetracyano-*p*-quinodimethane (TCNQ). TSeF-TCNQ has a slightly higher conductivity and a metal-insulator transition at lower temperature compared to TTF-TCNQ. The isostructurality of TSeF-TCNQ and TTF-TCNQ permits the formation of solid solutions $TSeF_xTTF_{1-x}TCNQ$ where x can be varied from 0 to 1. Solid solution compositions of single crystals, grown by slow cooling from saturated CH_3CN solutions. were determined by elemental analysis, x-ray analysis, and electron microprobe. and found to be homogeneous. Four-probe dc conductivity measurements as a function of temperature and powder x-ray measurements of the unit cell constants were carried out over the entire solid solution range.

While organic semiconducting charge-transfer salts have been known for some time,[1] the metallic state in an organic solid has only recently been discovered with the preparation of tetrathiafulvalene-tetracyano-*p*-quinodimethane (TTF-TCNQ, **1–2**).[2,3] TTF-TCNQ has been the subject of intense physical study and numerous new metal-like derivatives have been prepared.[4-7]

The origin of high conductivity in TTF-TCNQ derives from its segregated donor and acceptor stacked structure[8] (see Figure 1) and from incomplete charge-transfer which occurs between donor and acceptor stacks.[4,9,10] The quasi-one-dimensional structure of TTF-TCNQ makes this material prone to lattice distortions[4,11] (e.g., the Peierls instability) and at low temperature TTF-TCNQ undergoes at least two phase transitions[12] (53 and 38 K) which convert it into an insulator.

Attempts to correlate how modifications of the molecular constituents affect the metallic state in TTF-TCNQ are complicated by unpredictable changes that can occur in the crystal structure. Not only does one have to evaluate changes due to electronic perturbations on making a molecular modification, but also changes due to solid-state structural alterations. With the synthesis of the selenium analogues of TTF (e.g., tetraselenafulvalene[13] (TSeF, **3**) and diselenadithiafulvalene[14] (DSeDTF, **4**)),[15] electronic properties were perturbed[16] while still maintaining essentially the same steric requirements of the original TTF-TCNQ crystal structure.

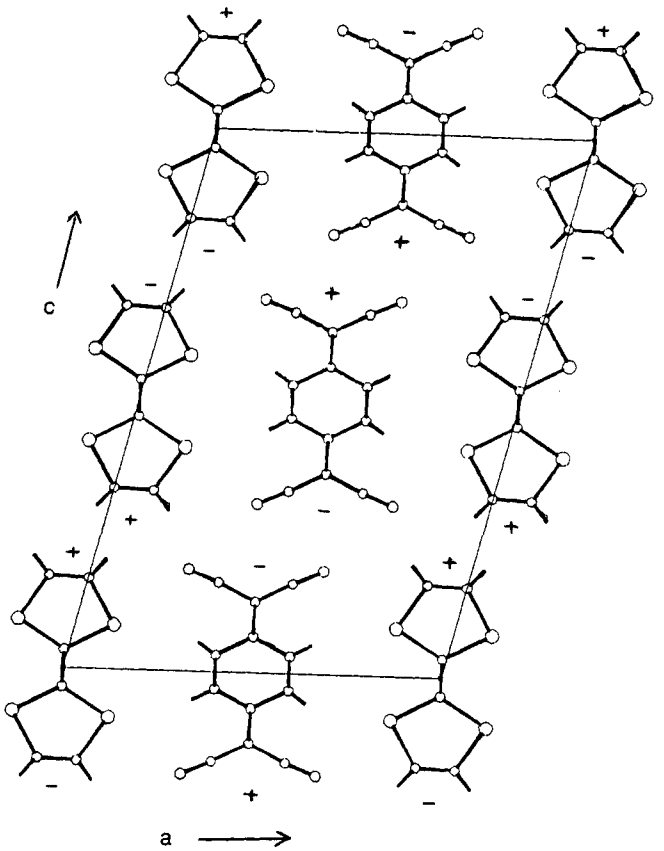

Figure 1. Projection of the *a*–*c* plane in TTF-TCNQ; the *b* axis is perpendicular to this plane, and plus and minus in the figure represent tilt of the molecules in the *a*–*c* plane.

Investigations of the properties of this isostructural family of organic metals (TTF-TCNQ, DSeDTF-TCNQ, TSeF-TCNQ) have provided important insights about the nature of the phase transitions which turn off the metallic state at low temperature and about the respective roles of the donor and acceptor stacks in determining overall solid-state properties.[12,17-22]

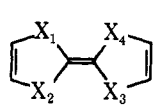

1, X_{1-4} = S
3, X_{1-4} = Se
4, $X_{1,3}$ = S; $X_{2,4}$ = Se
and $X_{1,4}$ = S; $X_{2,3}$ = Se

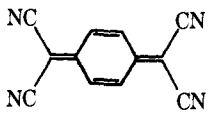

2

Another important feature of the close structural similarity between TSeF-TCNQ and TTF-TCNQ is that it permits, for the first time, the formation of solid solutions:[23] $TTF_xTSeF_{1-x}TCNQ$, where x can vary from 0 to 1, analogous to the alloying of two metals. These "organic alloys" provide a unique probe for the systematic modification of solid-state properties in which the character of the donor stack can be continuously varied from TTF to TSeF.

In this paper we describe the synthesis of the selenium analogues of TTF, the preparation and characterization of the solid solutions $TSeF_xTTF_{1-x}TCNQ$, and the general results of structural and electrical measurements on these systems. More detailed physical and theoretical treatments of these materials will appear elsewhere.[24]

Results and Discussion

Syntheses of the Selenium Analogues of TTF. The key synthetic precursor for preparing TTF and its derivatives is 1,3-dithiole-2-thione (**5**).[5] While a variety of synthetic methods are available for preparing **5**,[5] a simple one-step synthesis, developed by Mayer and Gebhardt,[25] seemed ideally suited for extension to selenium. Their procedure involved the addition of sulfur and carbon disulfide to sodium acetylide as shown in eq 1 (Y = X = S). In an analogous fashion, treatment of sodium acetylide with selenium and carbon diselenide yielded 1,3-diselenole-3-selone (**6**, Y = X = Se). However, when sulfur and carbon diselenide were added to sodium acetylide, not only was the expected product **7** formed (X = Se, Y = S), but a number of other related products were isolated as a result of scrambling of sulfur and selenium during the addition.[26]

Scheme I

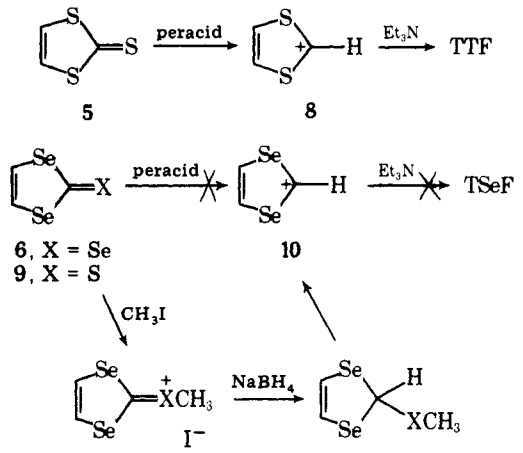

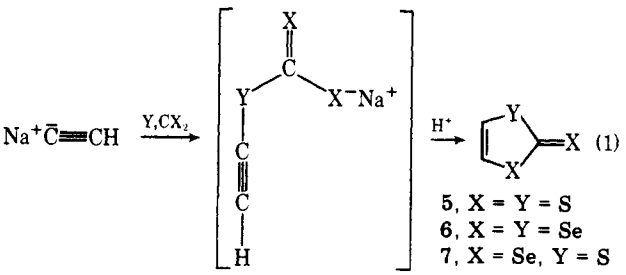

(1)

In the original TTF synthesis,[27] **5** was converted to TTF in two steps, involving peracid oxidation to the dithiolium salt (**8**),[28] followed by base coupling as shown in Scheme I. The analogous oxidation of **6** or **9**[26] fails to give the desired 1,3-diselenolium salt (**10**), probably due to attack of the ring seleniums during the oxidation.[29]

An alternate procedure for preparing **8** was recently developed by Wudl and co-workers[30] and was subsequently extended to the preparation of **10**.[31] However, **10** could not be coupled with alkylamine bases to give TSeF, as in the TTF synthesis. Elemental selenium rapidly precipitated from the reaction mixture on addition of base to **10**. Scheme I summarizes these reactions. While these differences between the organosulfur and -selenium chemistries in Scheme I frustrated our attempts to prepare TSeF by the published procedures for TTF, we were able to exploit another difference between sulfur and selenium to our advantage. Selenium forms weaker bonds to carbon than sulfur and, therefore, should be more easily removed using appropriate dechalcogenizing reagents such as trialkyl phosphites. Scheme II illustrates this point. With the selenocarbonyl precursor (**11**), TTF can be prepared in 60–70% yield, while only trace amounts of TTF, even under more strenuous reaction conditions, are detected starting with the thiocarbonyl derivative (**5**). Thus, the selenocarbonyl is the key to the effective coupling of the selenium analogues of TTF.[13,32,33] Reaction of selone **6** with trimethyl phosphite provided TSeF in good yield, while coupling of selone **7** gave

Table I. Molecular Properties of TTF, *cis-/trans*-DSeDTF, and TScF

Property	TTF	*cis-/trans*-DSeDTF	TSeF
MP, °C	119-119.5	117.0	132.5-133.0
UV-vis, λ(ε) (hexane)	303 (12 400)	297 (11 000)	287 (14 200)
	317 (11 000)	322 sh (6500)	300 sh (12 300)
	370 (1700)	375 sh (1000)	365 (1400)
	455 (250)	470 (175)	495 (130)
NMR (relative to Me_4Si, $CDCl_3$)	6.38	6.59, 6.95 (AB) J = 6.5 Hz 6.65, 6.89 (A'B') J = 6.5 Hz	7.25
Cyclic voltammetry[a] (CH_3CN, eV)	0.33, 0.70	0.40, 0.72	0.48, 0.76
g shift for donor radical cation	2.0084		2.027

[a] First and second peak oxidation potentials: for details see ref 16.

Scheme II

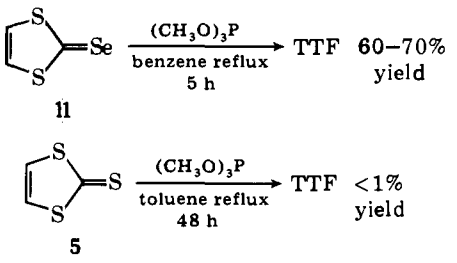

DSeDTF as an approximately equal mixture of cis and trans isomers as judged by NMR spectroscopy.[14]

Some physical properties of TTF, DSeDTF, and TSeF are summarized in Table I for comparison purposes. A shift of the longest visible absorption to lower energy on selenium incorporation is consistent with its assignment as a $\pi \rightarrow \pi^*$ transition.[27b,34] A rather large g shift is seen in going from $TTF^{+\cdot}$ to $TSeF^{+\cdot}$, due to the greater spin-orbit coupling for selenium. Interestingly, the selenium analogues of TTF are harder to ionize, despite the fact that selenium heterocycles tend to have lower ionization energies compared to their sulfur analogues.[16]

Solid Solution (Alloy) Formation and Characterization of $TSeF_xTTF_{1-x}TCNQ$. Single crystals of the charge-transfer salts of TTF and TSeF can be readily grown either by diffusion of the constituents together[35] or by slow cooling from saturated solutions. The latter method can give suitable crystals in less than a day, whereas the diffusion technique, while yielding perhaps better crystals, can take several weeks. Since solubility and diffusion differences between TSeF-TCNQ and TTF-TCNQ would tend to be more pronounced with the slower crystal growth technique, it was felt that more reproducible and uniform solid solution distributions could be realized by the slow cooling technique.

Three methods were employed to determine solid solution composition for $TSeF_xTTF_{1-x}TCNQ$: powder x-ray diffraction determination of the unit cell constants, elemental analysis, and electron microprobe measurements.[36] In the x-ray method, the alloy composition dependence of the unit cell constants is measured, and the results used to determine the composition of newly prepared alloy crystals. The a unit cell constant was employed as a composition guide, since it displays the largest increase of the unit cell constants and, as will be shown later, varies nearly linearly with solid solution composition.

Table II. Solid Solution Composition by Method

Initial composition[a]	x in $TSeF_xTTF_{1-x}TCNQ$			
		Elemental[c]	Electron microprobe[d]	
x_I	X ray[b]	analysis	Based on S	Based on Se
0.25	0.23	0.19	0.17	0.19
0.50	0.46	0.42	0.41	0.43
0.75	0.71	0.66	0.66	0.69
0.95	0.96	0.93	0.94	0.95

[a] Mole fraction TSeF in $TSeF_xTTF_{1-x}TCNQ$ used in crystal growth. [b] Based on expansion of a-axis unit cell parameter; see Figure 3. [c] Based on percent carbon. [d] Average of multiple determinations. See text for discussion.

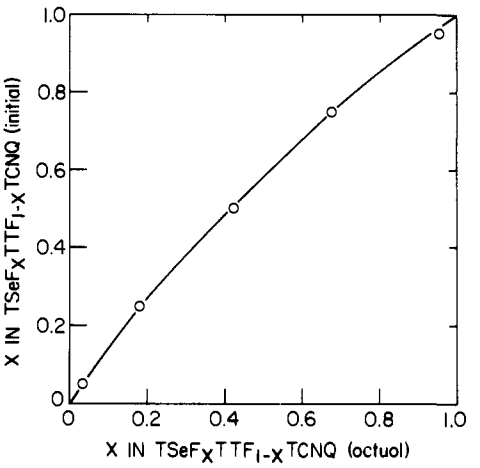

Figure 2. Plot of the initial solution composition (x_I) vs. the actual single crystal alloy composition (x) in $TSeF_xTTF_{1-x}TCNQ$.

The powder x-ray method, as well as elemental analysis, can consume a sizable portion of the single crystals grown in a typical crystallization experiment. Furthermore, these techniques do not provide information concerning composition homogeneity from crystal to crystal, or within an individual crystal. The electron microprobe method, on the other hand, can provide the mole fraction of sulfur and of selenium for the actual crystals upon which physical measurements, such as conductivity, are to be made. Regions (1 μm) can be probed routinely, permitting an analysis of the homogeneity of the solid solution composition along the length of an individual crystal as well as comparisons between different crystals.

In Table II, the three methods for determining solid solution composition are compared. Good agreement among the methods is obtained. In the electron microprobe measurements, both the sulfur and the selenium composition could be analyzed, giving two estimates of alloy composition. All three methods show an enrichment of alloy composition in TTF over that of the initial solution composition (x_I) except for $x = 0.95$, where values similar to the starting composition are obtained.

A plot of the initial solution composition (x_I) vs. the actual single-crystal alloy composition obtained (x) is given in Figure 2. With this plot, the initial solution composition needed to produce any desired alloy composition can be readily determined using conditions of crystal growth given in the Experimental Section.

In the electron microprobe measurement the Kα radiation from the sulfur and selenium atoms excited by an electron beam are counted for a given time interval. Ten points, in 2-μm steps along the crystal, were taken and averaged to give a single

Table III. Electron Microprobe Measurements on Solid Solutions

Initial composition x_1	$TSeF_xTTF_{1-x}TCNQ$ Electron microprobe composition $(x)^a$ Based on S	Based on Se	Comment
0.25	0.16	0.18	Three points in one crystal
	0.17	0.19	
	0.20	0.20	
0.95	0.93	0.98	Four points in one crystal
	0.93	0.96	
	0.94	0.97	
	0.92	0.94	
0.5	0.42	0.43	Four different crystals
	0.38	0.45	
	0.40	0.42	
	0.44	0.43	
0.75	0.66	0.68	Three different crystals
	0.67	0.70	
	0.64	0.68	
1	0	1.00	Pure TSeF-TCNQ
0	−0.03	0	Pure TTF-TCNQ
(0.50)[b]	0.48	0.53	Pure DSeDTF-TCNQ
	0.46	0.51	

[a] Individual values represent average on ten points taken in 2-μm steps. [b] This value is the mole fraction of selenium, Se/(Se + S). in DSeDTF, which is identical with the amount of selenium in the x = 0.50 solid solution sample.

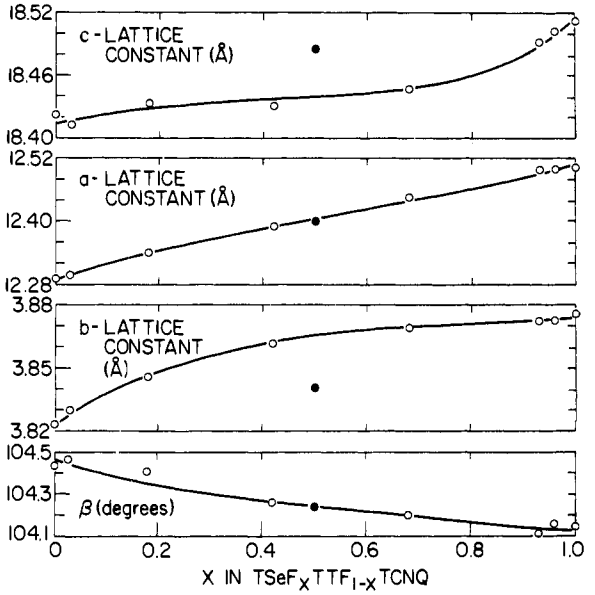

Figure 3. Plot of the monoclinic unit cell parameters a, b, c, and β as a function of x in $TSeF_xTTF_{1-x}TCNQ$. Solid points represent the values for DSeDTF-TCNQ.

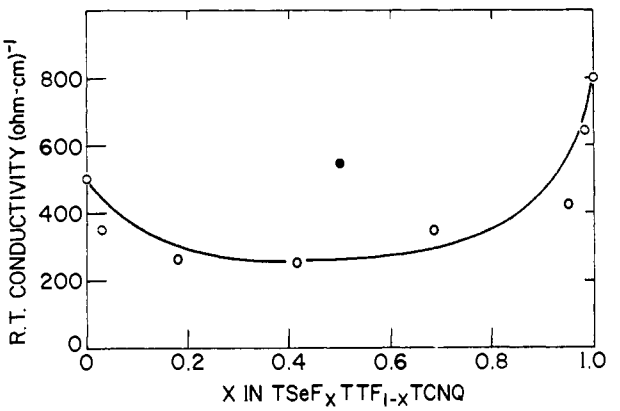

Figure 4. Plot of the room temperature conductivity (ohm cm)$^{-1}$ as a function of x in $TSeF_xTTF_{1-x}TCNQ$. Solid point represents DSeDTF-TCNQ. The accuracy of the conductivity values is estimated at ±100 (ohm cm)$^{-1}$.

determination of composition, typically with a precision of ±5% at 95% confidence level. Several such determinations of composition both at various points along a crystal and between crystals of a given batch were made, and averaged to give a final alloy composition listed in Table II (columns 4 and 5). Table III gives some representative data concerning the homogeneity of these solid solutions as judged by the electron microprobe technique. The composition values determined on an individual crystal (x_1 = 0.25 and 0.95) and between several crystals (x_1 = 0.50 and 0.75) indicate a fairly uniform solid solution distribution, within the experimental error of the technique. This error can be approximately gauged by the results of electron microprobe analysis on the pure TCNQ salts of TSeF, TTF, and DSeDTF, also listed in Table III.

Although the electron microprobe technique can only sample areas 1 μm in size, the narrowness of the line profiles in the x-ray diffraction patterns indicates a homogeneous distribution of TTF and TSeF in the donor stack on a microscopic scale. Detailed studies of electrical,[12,24] EPR,[18,37] and thermoelectric power[38] properties of these alloys also support a uniform alloy composition.

Structural Properties of $TSeF_xTTF_{1-x}TCNQ$. The variation in monoclinic unit cell parameters a, b, c, and β with x in $TSeF_xTTF_{1-x}TCNQ$ is given in Figure 3. These values were determined by indexing the powder x-ray diffraction patterns consistent with the space group $P2_1/c$ determined by single-crystal measurements on TTF-TCNQ[8] and on TSeF-TCNQ.[39] The smooth variation of these lattice constants lends confidence to their relative values over the entire solid solution range. Also included in Figure 3 are the same parameters for DSeDTF-TCNQ.

Figure 1 schematically illustrates the molecular relationships in the unit cell. All three lattice directions expand in going from TTF-TCNQ to TSeF-TCNQ. While the a-axis parameter varies nearly linearly with TSeF concentration, the b- and c-axis parameters vary nonlinearly and, interestingly, have their greatest rate of change occurring at opposite ends of the solid solution range. Only a rather small increase occurs in the b axis on TSeF incorporation, and the overall increase (0.05 Å) is considerably less than the expected van der Waals increase in going from sulfur to selenium (0.15-0.30 Å). The b axis is the stacking direction for these planar molecules, and represents the direction of strongest intermolecular overlap and highest conductivity. Thus, the rather small b-axis expansion suggests increased electronic overlap along the donor stacks in TSeF-TCNQ. On the other hand, this expansion also moves the TCNQ molecules apart, and would be expected to decrease their electronic overlap.

It is difficult to determine from the a-lattice parameter alone whether electronic overlap between donor and acceptor stacks has been enhanced in going from TTF-TCNQ to TSeF-TCNQ. However, complete crystal structure determinations on TTF-TCNQ[8] and TSeF-TCNQ[39] indicate stronger overlap of the chalcogen atom on the donor with the nitrogen on the acceptor, compared to the corresponding van der Waals distance (3.17 vs. 3.50 Å for TSeF-TCNQ and 3.25 vs. 3.35 Å for TTF-TCNQ, respectively).

Conductivity Results. The variation of the room temperature conductivity (σ_{rt}) with alloy composition, x, is given in Figure 4. The small number of samples measured for each alloy composition (three to four crystals) and the small span in conductivity values do not permit an accurate evaluation of σ_{rt}, except for TTF-TCNQ and TSeF-TCNQ where a much larger number of crystals were measured (18-20 crystals).

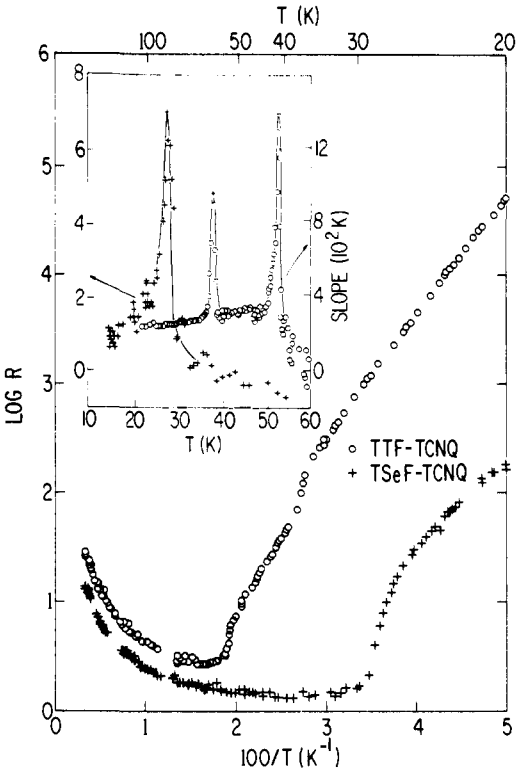

Figure 5. Plot of the log resistivity of TTF-TCNQ (O) and TSeF-TCNQ (+) vs. inverse temperature (K). Insert plots slope of log resistivity vs. temperature.

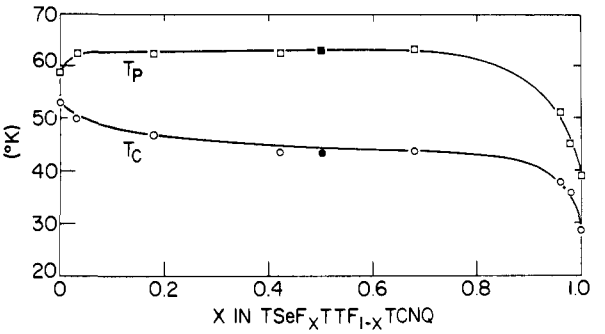

Figure 6. Plot of temperature of maximum conductivy, T_p (□), and phase transition temperature, T_c (O), as a function of x in $TSeF_xTTF_{1-x}TCNQ$. Solid points represents the values for DSeDTF-TCNQ.

However, the overall variation of σ_{rt} in Figure 4 should be qualitatively correct. The substitution of selenium for sulfur in TTF-TCNQ leads to an increase in the room temperature conductivity from a value of ~500 (ohm cm)$^{-1}$ for TTF-TCNQ to ~800 (ohm cm)$^{-1}$ for TSeF-TCNQ. At each end of the solid solution range, doping of the pure samples leads to a decrease in σ_{rt}. A broad minimum is reached near the middle of the solid solution range at which the conductivity is lower than either TTF-TCNQ or TSeF-TCNQ. A similar trend with alloy composition has been observed for the room temperature thermoelectric power.[38] Analysis of the thermoelectric power data[38] indicated that the disorder created in the donor stack due to the presence of TTF and TSeF selectively reduces the scattering time on the donor stack. Such an effect would lower conductivity when the donor stack makes a significant contribution to the overall conductivity.

A comparison of the σ_{rt} of DSeDTF-TCNQ (plotted in Figure 4, solid point) and that of a solid solution with $x = 0.5$ (interpolated from Figure 4) lends support for the above explanation.[38] Both systems have the same effective sulfur-selenium composition and have the donor stack randomly occupied by two different molecules. However, in the $x = 0.5$ solid solution, the donor stack is composed of TTF and TSeF, which have different ionization potentials (6.95 vs. 7.21 eV, respectively),[16] while in DSeDTF, the two molecules are cis and trans isomers with essentially the same ionization potentials.[16] One expects considerably less disruption of conductivity in DSeDTF-TCNQ than in $TSeF_{0.5}TTF_{0.5}TCNQ$ due to disorder, and this is seen experimentally, with σ_{rt} for DSeDTF-TCNQ twice as large as that for $TSeF_{0.5}TTF_{0.5}TCNQ$.

The effect of disorder due to alloy formation also manifests itself in a smaller increase in conductivity with decreasing temperature. The conductivity increases for the solid solutions by factors of 7-10 times in going from room temperature to the temperature T_p at which it peaks, compared to values for TTF-TCNQ and TSeF-TCNQ of 12-20 times σ_{rt}. A broadening of the conductivity peak in the alloys is also observed.

The behavior of the pure constituents (TTF-TCNQ and TSeF-TCNQ) in the transition region is contrasted in Figure 5, which shows the logarithm of the measured resistance vs. the inverse temperature.[12] The resistivity of TTF-TCNQ has a minimum at 59 K (T_p) and two major anomalies in the form of two sharp rises in resistivity at 53 and 38 K,[12] which correspond to actual phase transitions occurring in this material. These points are emphasized in the insert, which shows the slope of ln R vs. T. The two transitions manifest themselves as two sharp peaks over a smooth background. A third transition at 49 K had been predicted,[40] and subsequently found in neutron scattering experiments[41] and in a careful analysis of conductivity data.[42] In contrast to TTF-TCNQ, TSeF-TCNQ has a minimum at lower temperature (39 K) and only a single anomaly at 28 K.[12] In the insert, the single transition is seen as a somewhat broader peak.[43]

The variation of the temperature of maximum conductivity (T_p) and the phase transition temperature (T_c) over the entire solid solution range is given in Figure 6. The striking result of Figure 6 is the relative invariance of T_p and T_c over a rather large range of alloy composition, and the rapid change in value with the final replacement of the last few percent of TTF molecules with TSeF molecules. To emphasize this point, we note that nearly 50% of the total variation in T_c occurs over about the last 7% of the solid solution range.

A variety of solid-state measurements (e.g., EPR,[18,37] thermoelectric power,[38] conductivity,[12,17,24,44] optical reflectivity,[20] structural,[39] magnetic susceptibility,[22,45] and selective doping experiments[46,47]) all indicate a greater contribution of the donor to overall solid-state properties in TSeF-TCNQ than TTF-TCNQ. As discussed earlier, the structural parameters suggested enhanced overlap not only along the donor stack, but also between donor and acceptor stacks. This manifests itself in both a higher b- and a-axis conductivity for TSeF-TCNQ than for TTF-TCNQ.[44,48]

This increased electronic overlap between donor and acceptor stacks in TSeF-TCNQ is believed[12,18,49] to be important in the lowering of the temperature of the phase transition relative to TTF-TCNQ. While many factors are undoubtedly involved in controlling the phase transition, the role of interstack electronic coupling can be understood qualitatively as follows: The phase transitions in TTF-TCNQ and TSeF-TCNQ involve the interplay of dynamic lattice distortions (e.g., charge density waves) which occur on both donor and acceptor stacks. It is the building up of three-dimensional ordering of these charge density waves in certain phase relationships which brings about the transitions.[50-52] The energy gain for undergoing the phase transition is associated with the one-dimensional-like character of these materials (e.g., the Peierls instability). By making the system *less* one-dimensional, through

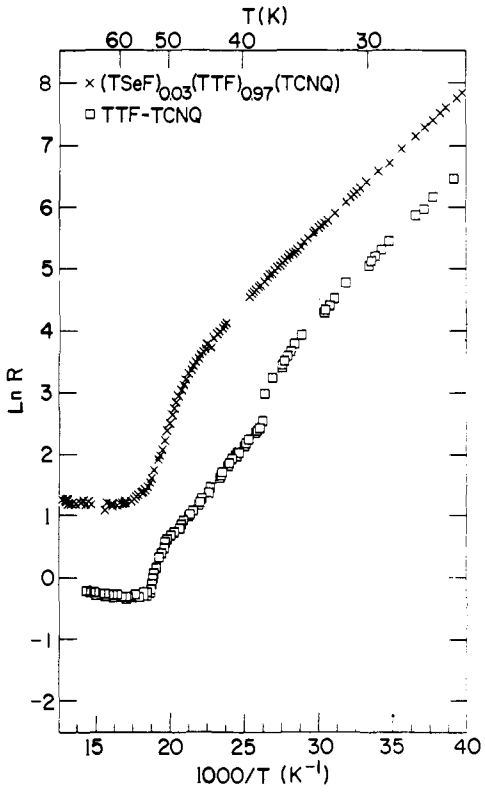

Figure 7. Plot of the log resistivity of TTF-TCNQ (□) and $TTF_{0.97}TSeF_{0.03}TCNQ$ (×) vs. inverse temperature (K^{-1}).

enhanced donor and acceptor stack electronic overlap, the energy gain for this transition to occur should be less and the transition shifted to lower temperature.[18,49,53]

Other factors may also be important in lowering T_c. The TCNQ stacks appear to play an important role in driving the phase transition by building up three-dimensional order in and between the TCNQ sheets (e.g., the *b*-*c* plane, Figure 1).[12,51] In going from TTF-TCNQ to TSeF-TCNQ, the TCNQ stacks are being pushed apart in both the *b*- and *c*-axis directions. These structural changes may also contribute to the lowering of T_c by decreasing the ability of the charge density waves on the acceptor stacks to three-dimensionally lock at the phase transition.[12,24,54]

More effective screening of charge density wave interactions between TCNQ stacks has also been proposed as a means of lowering T_c in going from TTF-TCNQ to TSeF-TCNQ.[52] Evaluation of the relative importance of all these factors in lowering T_c will have to await further study.

Insights have been gained concerning the unusual dependence of T_p and T_c with alloy composition from a study of the EPR line widths over the solid solution range.[18] A rather large increase in line width is found in going from TTF-TCNQ (5 G) to TSeF-TCNQ (500 G). After correcting for the contribution of greater spin-orbit coupling in selenium, considerable, additional relaxation of the signal remained at the high TSeF alloy compositions $x = 0.95, 0.98$ and for pure TSeF-TCNQ.[18] This extra relaxation was attributed to enhanced overlap between donor and acceptor stacks, and closely parallels the sharp decrease in T_c noted for these alloy compositions (Figure 6).

The enhanced electronic overlap between donor and acceptor stacks in TSeF-TCNQ may not only be involved in the lowering of T_c relative to TTF-TCNQ, but may also account for the apparent single transition that is observed in TSeF-TCNQ, as opposed to multiple transitions seen in TTF-TCNQ.[12] Considerable evidence has accumulated[47,51,55] which indicates that donor and acceptor stacks are weakly interacting in TTF-TCNQ, and that the metal-insulator transition at 53 K affects primarily the TCNQ stacks. The lower transitions at 49 and 38 K involve interactions on both donor and acceptor stacks.[11,40,51,55] With stronger interstack interaction in TSeF-TCNQ as well as enhanced overlap along the donor stack, both stacks seem to undergo their transition together.[24]

The effect of introducing small amounts of TSeF in TTF-TCNQ has been shown to be consistent with the above roles of the donor and acceptor stacks in the 53 and 38 K phase transitions.[12] Since the 53 K transition is believed to involve mainly the TCNQ stacks, it should be relatively unperturbed by a small amount of donor stack doping. On the other hand, the 38 K transition, which involves both donor and acceptor stacks, should be more sensitive to alloy formation. This is indeed the result: 3% incorporation of TSeF into TTF-TCNQ completely obscures the 38 K transition, while the 53 K transition remains relatively sharp (see Figure 7).[12]

Summary and Conclusion

The selenium analogues of TTF provide an unique approach for the systematic study of the metallic properties of TTF-TCNQ. In brief, some of the major findings of this work are:

(1) The key to the synthesis of TSeF and DSeDTF lies in the phosphite ester coupling of selenocarbonyl precursors **6** and **7**. The corresponding thiocarbonyl analogues cannot be coupled effectively this way or by the published procedures for TTF.

(2) Solid solutions or alloys of the isostructural organic metals, TSeF-TCNQ and TTF-TCNQ, can be routinely prepared for any desired value of x in $TSeF_xTTF_{1-x}TCNQ$. The electron microprobe technique is a convenient and reliable method of determining alloy composition on the actual single crystals upon which physical measurements are to be made.

(3) Powder X-ray diffraction measurements on the alloys indicate homogeneous distribution of TSeF and TTF on a microscopic level. The small expansion of the *a* and *b* lattice parameters suggests enhanced donor stack overlap in these directions in going from TTF-TCNQ to TSeF-TCNQ.

(4) Four-probe dc conductivity measurements yield a slightly higher *b*-axis conductivity in TSeF-TCNQ (σ_{rt} = 800/ohm cm) than in TTF-TCNQ (σ_{rt} = 500/ohm cm). Alloying decreases the room temperature conductivity, probably due to the effect of disordering the donor stack.

(5) The temperature of maximum conductivity (T_p) and the phase transition temperature (T_c) are surprisingly insensitive to large variation of alloy composition. Almost half of the decrease in T_c occurs in the last 7% replacement of TTF with TSeF (x = 0.93-1.00).

(6) The roles of the donor and acceptor stacks in the 53 and 38 K phase transitions could be probed by studying the alloys with small amounts of TSeF-TCNQ in TTF-TCNQ. These doping experiments support earlier studies[12,55] which indicate that the TCNQ stacks primarily drive the 53 K transition and that both donor and acceptor stacks are involved in the 38 K transition.

The present results support other studies on these materials[12,17-19,24,38] which indicate a stronger donor-acceptor stack electronic overlap (e.g., *a*-axis direction) in TSeF-TCNQ compared to TTF-TCNQ. This overlap is proposed to be important for lowering T_c in TSeF-TCNQ relative to TTF-TCNQ, and together with enhanced donor overlap in the solid may account for the single phase transition in TSeF-TCNQ compared to several in TTF-TCNQ. It is noted that the pushing apart of the TCNQ stacks in the *b* and *c* lattice directions in going from TTF-TCNQ to TSeF-TCNQ may also be involved in lowering T_c. Further study is necessary before the relative importance of these contributions, as well as other

factors, in determining solid-state properties can be evaluated with confidence.

Experimental Section

Synthetic. (A) Preparation of 1,3-Diselenole-2-selone (6). A procedure similar to that described in ref 26 was employed to prepare **6** in yields ranging from 10 to 20%. Extreme caution should be exercised in handling the highly toxic and odorous carbon diselenide. Carbon diselenide can be conveniently and reproducibly prepared in large batches by the detailed procedure of Henriksen and Kristiansen.[56] After the preparation of sodium acetylide and the addition of selenium, it is important to remove as much of the ammonia solvent as possible, since the next step involves the addition of carbon diselenide, which is known to polymerize in the presence of ammonia. Chromatography may be necessary if oiling of the product from the methylcyclohexane extracts is a problem. Typically, the crude product is placed on a long silica gel column and eluted with large amounts of hexane, in order to remove nonpolar impurities. The product is moved down the column with 20% $CHCl_3$–hexane. Crystallization from hexane gives purple-red needles of **6**, mp 106–108 °C.[26]

In a similar fashion, 1,3-thiaselenole-2-selone (**7**) could be prepared. In this case, a mixture of products is obtained and a more careful chromatography using 5% $CHCl_3$–CCl_4 is necessary.[26]

(B) Preparation of Tetraselenafulvalene (3). Into a 50-mL round-bottom flask equipped with a heating mantle, reflux condenser, magnetic stirrer, and nitrogen bubbler was placed 0.80 g (3 mmol) of 1,3-diselenole-2-selone in 25 mL of dry benzene and 0.80 g (6 mmol) of trimethyl phosphite. The reaction mixture was refluxed several hours under nitrogen and the solvent evaporated on a rotary evaporator. The residual dark brown reaction mixture was dissolved in a minimal amount of chloroform–hexane and placed over a 1 ft × 1 in. silica gel column. Elution with hexane moved the product down the column, and TSeF crystallized from hexane as red crystals (yield 50–60%). The crystallization procedure should be carried out under N_2 to minimize product loss due to oxidation to the TSeF radical cation. TSeF can be further purified by gradient sublimation at 10–20 μm and 60 °C (bath temperature).

Similarly, diselenadithiafulvalene (**4**) could be prepared by coupling 1,3-thiaselenole-2-selone (**7**). Table I summarizes some of the physical properties of TSeF and DSeDTF in comparison with the values for TTF.

(C) Solid Solution Preparations: $TSeF_xTTF_{1-x}TCNQ$. The neutral components, TTF, DSeDTF, TSeF, and TCNQ, were purified[57] by three cycles of recrystallization–gradient sublimation with the last cycle being carried out in an inert atmosphere box (Argon). TTF, DSeDTF, and TSeF were recrystallized from isooctane (Burdick and Jackson grade). The acetonitrile (Burdick and Jackson grade), used to recrystallize TCNQ and for crystal growing, was purifed by distillation from P_2O_5 through a 3-ft glass-packed column under N_2.

All crystal growing was preformed in a drybox (Argon) where H_2O and O_2 were maintained at <1 ppm. In a typical crystal growth experiment, the weighed components (~0.1 mmol each of donor and of acceptor) were dissolved in hot acetonitrile (20–25 mL), filtered into a stoppered flask, placed hot into a preheated Dewar, and packed with warmed glass wool. Overnight standing at room temperature usually gave long black, needle-like crystals suitable for conductivity measurements. The filtered crystals were washed with hexane and stored under N_2 before use.

Structural Measurements. X-ray diffraction of the powdered crystals was used to determine the crystallographic parameters using the fully determined crystal structure of TTF–TCNQ. The structural parameters for the entire solid solution range (x = 0–1) were determined by a least-squares indexing of the Guinier x-ray powder patterns (Cu Kα radiation) using reflections in the range 2θ = 20–60°. No nonindexable reflections were observed, and the narrowness of the line profiles indicated high sample homogeneity.

Conductivity Measurements. The dc conductivity was measured by a standard four probe dc method.[58] The data were taken with a computer-controlled device, a procedure that was found to be essential in collecting a large ensemble of data and its easy manipulation. For details see ref 24.

Acknowledgments. The authors thank S. Ellman, F. Cardone, and J. Kuptsis of the IBM Research Center for carrying out the electron microprobe measurements. We are grateful to Drs. Y. Tomkiewicz, R. A. Craven, and T. D. Schultz from IBM and to Professor P. M. Chaikin from UCLA for many stimulating discussions which have helped shape some of the ideas presented here. Dr. S. La Placa's help in providing Figure 1 is gratefully acknowledged.

References and Notes

(1) See for example: F. Gutman and L. E. Lyons, "Organic Semiconductors", Wiley, New York, N.Y., 1967.
(2) J. Ferraris, D. O. Cowan, V. Walatka, Jr., and J. H. Perlstein, *J. Am. Chem. Soc.*, **95**, 948 (1973); L. B. Coleman, M. J. Cohen, D. J. Sandman, F. G. Yamagishi, A. F. Garito, and A. J. Heeger, *Solid State Commun.*, **12**, 1125 (1973).
(3) For a recent discussion of the electrical properties of TTF–TCNQ from two points of view see: G. A. Thomas et al., *Phys. Rev. B*, **13**, 5105 (1976); M. J. Cohen, L. B. Coleman, A. F. Garito, and A. J. Heeger, *ibid.*, **13**, 5111 (1976).
(4) Reviews: (a) A. F. Garito and A. J. Heeger, *Acc. Chem. Res.*, 7, 232 (1974); (b) A. N. Bloch, D. O. Cowan, and T. O. Poehler in "Energy and Charge Transfer in Organic Semiconductors", K. Masuda and M. Silver, Ed., Plenum Publishing Co., New York, N.Y., 1974; (c) A. J. Heeger and A. F. Garito in "Low Dimensional Cooperative Phenomena", H. J. Keller, Ed., Plenum Publishing Co., New York and London, 1975; (d) A. J. Berlinsky, *Contemp. Phys.*, **17**, 331 (1976); (e) E. M. Engler, *CHEMTECH*, **6**, 274 (1976).
(5) Review of TTF modifications: M. Narita and C. U. Pittman, Jr., *Synthesis*, 489 (1976).
(6) Recent TCNQ modifications: R. C. Wheland and E. L. Martin, *J. Org. Chem.*, **40**, 3101 (1975); see also B. P. Bespalov and V. V. Titov, *Russ. Chem. Rev.*, **44**, 1091 (1975).
(7) Recent references on new organic conductors not included in above reviews: R. C. Wheland and J. L. Gillson, *J. Am. Chem. Soc.*, **98**, 3916 (1976); R. C. Wheland, *ibid.*, **98**, 3926 (1976); C. S. Jacobsen, J. R. Andersen, K. Bechgaard, and C. Berg, *Solid State Commun.*, **19**, 1209 (1976); C. Berg, K. Bechgaard, J. R. Andersen, and C. S. Jacobsen, *Tetrahedron Lett.*, 1719 (1976); M. L. Khidekel and E. B. Yagubskii, *Bull. Acad. Sci., USSR, Div. Chem. Sci.*, 1123 (1975); F. Wudl, D. E. Schafer, and B. Miller, *J. Am. Chem. Soc.*, **98**, 252 (1976); A. J. Schultz, G. D. Stucky, R. A. Craven, M. J. Schaffman, and M. B. Salamon, *ibid.*, **98**, 5191 (1976).
(8) T. J. Kistenmacher, T. E. Phillips, and D. O. Cowan, *Acta Crystallogr., Sect. B*, **30**, 763 (1974).
(9) W. D. Grobman, R. A. Pollak, D. E. Eastman, E. T. Maas, Jr., and B. A. Scott, *Phys. Rev. Lett.*, **32**, 534 (1974); J. B. Torrance and B. D. Silverman, *Phys. Rev. B*, **15**, 788 (1977); S. J. La Placa, P. W. Corfield, R. Thomas, and B. A. Scott, *Solid State Commun.*, **17**, 635 (1975).
(10) Electron–electron correlations have been proposed as important in determining the properties of these materials: J. B. Torrance, B. A. Scott, and F. B. Kaufman, *Solid State Commun.*, **17**, 1369 (1975); J. B. Torrance, "Proceedings of NATO Advanced Study Institute on Chemistry and Physics of One-Dimensional Metals", Bolzano, Italy, Aug 1976, H. J. Keller, Ed., Plenum Publishing Co., New York, N.Y., 1977. For an alternate point of view see ref 4c.
(11) For recent x-ray and neutron scattering measurements of these lattice distortions: F. Denoyer, R. Comès, A. F. Garito, and A. J. Heeger, *Phys. Rev. Lett.*, **35**, 445 (1975); S. Kagoshima, H. Arazi, K. Kajimura, and T. Ishiguro, *J. Phys. Soc. Jpn.*, **39**, 1143 (1975); R. Comès, S. M. Shapiro, G. Shirane, A. F. Garito, and A. J. Heeger, *Phys. Rev. Lett.*, **35**, 1518 (1975); R. Comès, G. Shirane, S. M. Shapiro, A. F. Garito, and A. J. Heeger, *Phys. Rev. B.*, **14**, 2376 (1976).
(12) S. Etemad, *Phys. Rev. B*, **13**, 2254 (1976). For the second transition in TTF–TCNQ, see also references cited therein.
(13) E. M. Engler and V. V. Patel, *J. Am. Chem. Soc.*, **96**, 7376 (1974).
(14) E. M. Engler and V. V. Patel, *J. Chem. Soc., Chem. Commun.*, 671 (1975).
(15) Alternate syntheses of TSeF and DSeDTF have appeared: M. V. Lakshmikanthan and M. P. Cava, *J. Org. Chem.*, **41**, 882 (1976); M. V. Lakshmikanthan, M. P. Cava, and A. F. Garito, *J. Chem. Soc., Chem. Commun.*, 383 (1975).
(16) E. M. Engler, F. B. Kaufman, D. C. Green, D. E. Klots, and R. N. Compton, *J. Am. Chem. Soc.*, **97**, 2921 (1975).
(17) S. Etemad, T. Penney, E. M. Engler, B. A. Scott, and P. E. Seiden, *Phys. Rev. Lett.*, **34**, 741 (1975).
(18) Y. Tomkiewicz, E. M. Engler, and T. D. Schultz, *Phys. Rev. Lett.*, **35**, 456 (1975).
(19) P. M. Chaikin, R. L. Greene, S. Etemad, and E. M. Engler, *Phys. Rev. B*, **13**, 1627 (1976).
(20) B. Welber, E. M. Engler, P. M. Grant, and P. E. Seiden, *Bull. Am. Phys. Soc.*, **35**, 311 (1976).
(21) C. Weyl, E. M. Engler, K. Bechgaard, G. Jehanno, and S. Etemad, *Solid State Commun.*, **19**, 925 (1976).
(22) S. Etemad, T. Penney, and E. M. Engler, *Bull. Am. Phys. Soc.*, **20**, 496 (1975).
(23) Presented in part: E. M. Engler, S. Etemad, T. Penney, and B. A. Scott, 169th National Meeting of the American Chemical Society, Philadelphia, Pa., April 8, 1975, Abstract ORGN 43; S. Etemad, E. M. Engler, B. A. Scott and T. Penney, *Bull. Am. Phys. Soc.*, **20**, 496 (1975).
(24) S. Etemad, E. M. Engler, T. Penney, B. A. Scott, and T. D. Schultz, *Phys. Rev. B*, submitted for publication.
(25) R. Mayer and B. Gebhardt, *Chem. Ber.*, **97**, 1298 (1964).
(26) E. M. Engler and V. V. Patel, *J. Org. Chem.*, **40**, 387 (1975).
(27) (a) F. Wudl, G. M. Smith and E. J. Hufnagel, *Chem. Commun.*, 1435 (1970); (b) D. L. Coffen, J. Q. Chambers, D. R. Williams, P. E. Garrett and N. D. Canfield, *J. Amer. Chem. Soc.*, **93**, 2258 (1971); (c) S. Hünig, G. Kiesslich, H. Quast, and D. Scheutzow, *Justus Liebigs Ann. Chem.*, 310 (1973).

(28) E. Klingsberg, *J. Amer. Chem. Soc.*, **86**, 5290 (1964).
(29) In a related reaction, oxidation of 1,3-diselenane under similar conditions yields the corresponding 1,4-dioxide; E. S. Gould and W. Burlant, *J. Amer. Chem. Soc.*, **78**, 5825 (1956).
(30) F. Wudl, M. L. Kaplan, E. J. Hufnagel and E. W. Southwick, Jr., *J. Org. Chem.*, **39**, 3608 (1974).
(31) E. M. Engler and V. V. Patel, *Tetrahedron Lett.*, 1259 (1975).
(32) Phosphorus base coupling is currently the only effective means of coupling the selenium analogues of TTF. See ref 5 for discussion. See also: H. K. Spencer, M. V. Lakshmikantham, M. P. Cava, and A. F. Garito, *J. Chem. Soc., Chem. Commun.*, 867 (1975). It is also important to note that 4,5-disubstituted 1,3-diselenoles require the selone substituent; thione derivatives lead to scrambling of sulfur and selenium. For details see: E. M. Engler, R. R. Schumaker, and V. V. Patel, *ibid.*, submitted for publication.
(33) A convenient procedure for converting thiocarbonyl 1,3-dichalcogenole derivatives to the corresponding selenocarbonyl compounds has recently been reported: E. M. Engler and V. V. Patel, *Tetrahedron Lett.*, 423 (1976).
(34) R. Gleiter, M. Kobayashi, J. Spanget-Larsen, J. P. Ferraris, A. N. Bloch, K. Bechgaard, and D. O. Cowan., *Ber. Bunsen ges. Phys. Chem.*, **79**, 1224 (1975); R. Gleiter, E. Schmidt, D. O. Cowan, and J. P. Ferraris, *J. Electron Spectrosc. Relat. Phenom.*, **2**, 207 (1973).
(35) G. T. Pott and J. Kommandeur, *Mol. Phys.*, **13**, 373 (1967); M. L. Kaplan, *J. Cryst. Growth*, **33**, 161 (1976). H. Anzai, *ibid.*, **33**, 185 (1976).
(36) For an overview of this method see: "Microprobe Technique", C. A. Andersen. Ed., Wiley, New York, N.Y., 1973.
(37) Y. Tomkiewicz, A. R. Taranko, and E. M. Engler, *Phys. Rev. Lett.*, **37**, 1705 (1977).
(38) P. M. Chaikin, J. F. Kwak, R. L. Greene, S. Etemad, and E. M. Engler, *Solid State Commun.*, **19**, 954 (1976).
(39) S. J. La Placa and P. W. Corfield, unpublished work.
(40) P. Bak and V. J. Emery, *Phys. Rev. Lett.*, **36**, 978 (1976).
(41) W. D. Ellenson, R. Comès, S. M. Shapiro, G. Shirane, A. F. Garito, and A. J. Heeger, submitted for publication.
(42) R. A. Craven, S. Etemad, T. Penney, P. M. Horn, and D. Guidotti, unpublished work.
(43) A second "impurity" transition has been observed: R. A. Craven, Y. Tomkiewicz, E. M. Engler, and A. R. Taranko, *Solid State Commun.*, in press.
(44) J. R. Cooper, D. Jérome, S. Etemad, and E. M. Engler, *Solid State Commun.*, **22**, 257 (1977).
(45) J. C. Scott, S. Etemad, and E. M. Engler, *Solid State Commun.*, submitted for publication.
(46) E. M. Engler, R. A. Craven, Y. Tomkiewicz, B. A. Scott, K. Bechgaard and J. R. Andersen, *J. Chem. Soc., Chem. Commun.*, 337 (1976).
(47) Y. Tomkiewicz, R. A. Craven, T. D. Schultz, E. M. Engler, and A. R. Taranko, *Phys. Rev. B*, **15**, 1011 (1977).
(48) D. Guidotti, P. Horn, and E. M. Engler, "Proceedings of the Conference on Organic Conductors and Semiconductors", Siofok, Hungary, Aug 30–Sept 3, 1976.
(49) Y. Tomkiewicz and T. D. Schultz, submitted for publication.
(50) M. J. Rice and S. Strassler, *Solid State Commun.*, **13**, 1385 (1975); P. A. Lee, T. M. Rice and P. W. Anderson, *Phys. Rev. Lett.*, **31**, 462 (1973).
(51) T. D. Schultz and S. Etemad, *Phys. Rev. B*, **13**, 4928 (1976).
(52) T. D. Schultz, *Solid State Commun.*, **22**, 289 (1977).
(53) In HMTSF–TCNQ, an alkyl-substituted derivative of TSeF–TCNQ, donor–acceptor stack interactions may be even stronger and this may account for the unusual low-temperature behavior of this material. For details see: A. N. Bloch, D. O. Cowan, K. Bechgaard, R. E. Pyle, R. H. Banks, and T. O. Poehler, *Phys. Rev. Lett.*, **34**, 1561 (1975); J. R. Cooper, M. Weger, D. Jérome, D. Lefur, K. Bechgaard, A. N. Bloch, and D. O. Cowan, *Solid State Commun.*, **19**, 749 (1976); M. Weger, *ibid.*, **19**, 1149 (1976); G. Soda, D. Jérome, M. Weger, K. Bechgaard, and E. Pedersen, *ibid.*, **20**, 107 (1976).
(54) In a series of TTF charge transfer salts, it was found that increasing the intrastack separations in the TTF stack led to a decrease in T_c: G. A. Thomas, F. Wudl, F. DiSalvo, W. M. Walsh, Jr., L. W. Rupp, and D. E. Schafer, *Solid State Commun.*, **20**, 1009 (1976).
(55) Y. Tomkiewicz, A. R. Taranko, and J. B. Torrance, *Phys. Rev. Lett.*, **36**, 751 (1976); E. F. Rybaczewski, A. F. Garito, A. J. Heeger, and E. Ehrenfreund, *ibid.*, **34**, 524 (1975); E. F. Rybaczewski, L. S. Smith, A. F. Garito, and A. J. Heeger, *Phys. Rev. B*, **14**, 2746 (1976); M. Barmatz, L. R. Testardi, A. F. Garito, and A. J. Heeger, *Solid State Commun.*, **15**, 1299 (1974).
(56) L. Henriksen and E. S. Kristiansen, *Int. J. Sulfur Chem. A.*, **2**, 13 (1972).
(57) For a discussion of the effect of chemical purity on electrical properties see: R. V. Gemmer, D. O. Cowan, T. O. Poehler, A. N. Bloch, R. E. Pyle, and R. H. Banks, *J. Org. Chem.*, **40**, 3544 (1975).
(58) For information on the technique of conductivity measurements on organic conductors see: L. B. Coleman, *Rev. Sci. Instrum.*, **46**, 1125 (1976).

The Transition State for Exchange of Protons and Metal Ions in a Carboxylate Ion-Exchange Resin[1]

Julio F. Mata Segreda, Siegfried Lindenbaum, and Richard L. Schowen*

Contribution from the Departments of Chemistry and Pharmaceutical Chemistry, University of Kansas, Lawrence, Kansas 66045, and the School of Chemistry, University of Costa Rica, San José, Costa Rica. *Received February 7, 1977*

Abstract: The release of protons from Amberlite CG-50 ion-exchange resin into water at 25.0 ± 0.5 °C, induced by lithium, sodium, or potassium ions, is a first-order process with a rate constant of $7.4 \pm 0.4 \times 10^{-3}$ s^{-1}. This constant is independent of metal-ion concentration and identity, quantity of resin, and stirring speed under the conditions employed. The rate constant for proton release into protium oxide exceeded that for deuteron release into deuterium oxide by factors of 3.06 ± 0.17 (Na^+) and 3.36 ± 0.38 (K^+). The rate constant k_n for lyon release into binary mixtures of protium oxide and deuterium oxide (atom fraction n of deuterium) is given by the equation $k_n = (7.4 \pm 0.5 \times 10^{-3}\ s^{-1})(1 - n + [0.70 \pm 0.02]n)^3$. The transition state for proton release from the resin appears to be that for migration of a preformed hydronium ion through the resin matrix. This migration generates a hole which is rapidly occupied by the metal ion.

The exchange of protons and metal ions at macromolecular binding sites is a process of considerable importance in a variety of fields, not least in biochemistry.[2] A simple system susceptible of kinetic study[3] is offered by ion-exchange resins. We report here solvent isotope effect studies which permit a characterization of some features of the transition state for proton release from a carboxylate resin, induced by alkali-metal cations.

Results

These studies were conducted by monitoring the pH of a stirred aqueous solution in contact with a quantity of Amberlite CG50 ion exchange resin, hereafter called "resin". When alkali-metal chlorides were added to the aqueous phase, protons were slowly released from the resin and the pH decreased. No slow proton release was observed from resin in contact with water not containing alkali-metal salts. The release of protons was a first-order process, as the data of Figure 1 demonstrate, after an initial 1–2 min period of swelling and equilibration. The total number of protons released when the external metal-ion concentration was around 0.1 M constituted about 3% of the protons titratable by sodium hydroxide.

Effect of Stirring Speed and Quantity of Resin. With 0.1 M external sodium chloride concentration, the stirring speed was maintained at 1120, 2310, and 3060 rpm and rate constants for proton release 7.41 ± 0.41, 7.40 ± 0.54, and 7.41 ± 0.17 $\times 10^{-3}$ s^{-1}, respectively, were obtained. Thus, in this range, the rate constant for proton release is unaffected by stirring

* Address correspondence to this author at the University of Kansas.